ApJ Letters, in press

Do young galaxies exist in the Local Universe? — Red Giant Branch detection in the metal-poor dwarf SBS 1415+437[1]

A. Aloisi[2,3], R. P. van der Marel[2], J. Mack[2], C. Leitherer[2], M. Sirianni[2,3] and M. Tosi[4]

ABSTRACT

We present results from an HST/ACS imaging study of the metal-poor blue compact dwarf galaxy SBS 1415+437. It has been argued previously that this is a very young galaxy that started to form stars only $\lesssim 100$ Myr ago. However, we find that the optical color-magnitude diagram prominently reveals asymptotic giant branch and red giant branch (RGB) stars. The brightness of the RGB tip yields a distance $D \approx 13.6$ Mpc. The color of the RGB implies that its stars must be older than ~ 1.3 Gyr, with the exact age depending on the assumed metallicity and dust extinction. The number of RGB stars implies that most of the stellar mass resides in this evolved population. In view of these and other HST results for metal-poor galaxies it seems that the local Universe simply may not contain any galaxies that are currently undergoing their first burst of star formation.

Subject headings: galaxies: dwarf — galaxies: irregular — galaxies: evolution — galaxies: individual (SBS 1415+437) — galaxies: stellar content

---

[1]Based on observations with the NASA/ESA Hubble Space Telescope, obtained at the Space Telescope Science Institute, which is operated by AURA for NASA under contract NAS5-26555.

[2]Space Telescope Science Institute, 3700 San Martin Drive, Baltimore, MD 21218; aloisi@stsci.edu, marel@stsci.edu, mack@stsci.edu, leitherer@stsci.edu, sirianni@stsci.edu

[3]On assignment from the Space Telescope Division of the European Space Agency.

[4]INAF-Osservatorio Astronomico di Bologna, Via Ranzani 1, I-40127 Bologna, Italy; monica.tosi@bo.astro.it

1. Introduction

Within the framework of hierarchical formation, dwarf ($M \lesssim 10^9$ $M_\odot$) galaxies are often considered the first systems to collapse, supplying the building blocks for the formation of more massive galaxies through merging and accretion. So present-day dwarfs may have been sites of the earliest star-formation (SF) activity in the Universe. However, this hypothesis is challenged by the physical properties of blue compact dwarf (BCD) galaxies, which have blue colors indicative of a young stellar population. BCDs are experiencing intense SF (0.01-10 $M_\odot$ yr^{-1}; Thuan 1991) but still have a high neutral gas content ($\gtrsim 10^8$ $M_\odot$; Thuan & Martin 1981). Oxygen abundances in H II regions generally imply a low metal content, with values in the range $12 + \log(O/H) = 7.1$–8.3 (Izotov & Thuan 1999; hereafter IT99). Some BCDs contain much less heavy elements than the majority of high-z galaxies. The most metal-poor BCDs ($12 + \log(O/H) \lesssim 7.6$) have therefore been pointed out as particularly good candidate "primeval" galaxies in the nearby Universe that started to form stars no more than 40 Myr ago (IT99). This would support the view that SF in low-mass systems has been inhibited until the present epoch (Babul & Rees 1992). In any case, chemically poorly evolved star-forming dwarfs are the best laboratory where to study SF processes similar to those occurring in the early Universe, but with a spatial resolution and sensitivity that are impossible to achieve in high-z galaxies.

The most direct way to infer the age of a nearby galaxy is to resolve it into individual stars and study the color-magnitude diagram (CMD). The red giant branch (RGB) sequence, formed by evolved stars with ages in excess of ~ 1 Gyr, is of particular interest. An unambiguous RGB detection implies that SF was already active more than a Gyr ago, whereas absence of the RGB indicates that the system has started forming stars only recently. Here we report results from a new V and I-band imaging study of the metal-poor BCD SBS 1415+437, performed with the Hubble Space Telescope (HST) Advanced Camera for Surveys (ACS).

Together with I Zw 18 (see Section 4), SBS 1415+437 may be one of the best candidate primeval galaxies in the local Universe. It has an elongated shape with a bright H II region at its SW tip (see Figure 1). The systemic velocity corrected for Local Group infall towards Virgo is 851 $km\,s^{-1}$ (from the Lyon Extragalactic Database). Ignoring any possible peculiar velocity, this implies a distance $D = 12.2$ Mpc and an intrinsic distance modulus $m - M = 30.42$ for $H_0 = 70\,km\,s^{-1}\,Mpc^{-1}$. The galaxy has an oxygen abundance $12 + \log(O/H) = 7.59 \pm 0.01$ (IT99) and was studied in considerable detail by Thuan, Izotov, & Foltz (1999, hereafter T99). It has a blue integrated color, $V - I \lesssim 0.4$ throughout the main body, indicating that young stars are dominating its light. Its SF regions were studied through UV and optical spectroscopy, stellar population synthesis modeling and chemical abundance

determination. T99 concluded from all the combined evidence that SBS 1415+437 is a young galaxy that did not start to make stars until $\sim$ 100 Myr ago. T99 also presented HST/WFPC2 data that resolved the brightest young stars, but these data were too shallow (1800 sec in V and 4400 sec in I) to reach evolved asymptotic giant branch (AGB) or RGB stars.

2. Observations and Data Reduction

SBS 1415+437 was observed in HST GO program 9361 using the ACS Wide Field Channel (WFC). The full field of view is $\sim 200 \times 200$ arcsec^2 with a pixel size of 0.05×0.05 arcsec^2. Total integration times of 20160 sec were obtained for each of the filters F606W and F814W. The 16 optimally dithered single exposures per filter were reprocessed with the most up-to-date version of the ACS calibration pipeline. The exposures were registered, corrected for geometric distortion, and co-added with cosmic-ray rejection using the `MultiDrizzle` software. Figure 1 shows a true color image created by combining the data from the two filters.

Point source photometry was performed with the `DAOPHOT/ALLSTAR` package (Stetson 1987). A spatially variable point-spread function (PSF) was inferred from the most isolated stars in the target vicinity and was fitted to the detected stars within the galaxy. A master catalog was created by matching peaks in excess of 4σ in a sum of the V and I images, yielding $\sim$ 21000 detected objects. Because of the large number of dithered exposures, the master catalog is essentially free of instrumental artifacts such as cosmic rays or hot pixels. The vast majority of the detected sources are individual stars in the galaxy, with a small potential contamination from stars blends and background galaxies (foreground star contamination is predicted to be negligible). We did not remove potentially contaminating sources from our catalog by applying cuts in sharpness or χ^2, so as to not run the risk of rejecting bona fide stars in SBS 1415+437 as well. However, we did experiment with rejection strategies of various kinds and found that none of the results presented here depend on this aspect of the analysis.

Photometry was performed at the positions of the objects in the master catalog separately in the V and I band images. Aperture corrections were measured from stars in the frame, and applied to all photometry. Corrections for imperfect Charge Transfer Efficiency (CTE) were applied based on extrapolation of the calibration of Riess & Mack (2004). Contamination to F606W by extended Hα emission was corrected in the photometric analysis through local background subtraction. Count rates were transformed to the Johnson-Cousins V and I magnitudes using the color-dependent synthetic transformations given by Sirianni

et al. (2005), which have been shown to be accurate to ~ 0.02 mag.

Figure 2a shows the inferred $(V-I,\ I)$ CMD for the full area of the sky covered by the galaxy. The median random errors in the photometry are indicated in the figure. These errors do not account for the possible influence of star blending, which will generally add additional systematic uncertainties. An estimate of the 50% completeness limit is also shown in the figure. This estimate was obtained by fitting the combination of a parameterized completeness function and a model SF history to the observed CMD. The resulting estimate is an average over the galaxy, given that the actual completeness varies spatially depending on the level of crowding. The simple estimates of the errors and completeness in Figure 2a suffice for the purposes of the present paper. In a forthcoming follow-up paper we will present artificial star tests to estimate these quantities more robustly, and also as function of position in the galaxy. That paper will also contain more details about the data reduction and photometric analysis, and will discuss narrow-band imaging obtained in the context of the same HST program.

3. CMD Analysis

At bright magnitudes in the CMD ($I \lesssim 25$) we find the same star types detected previously with WFPC2 (T99): main sequence stars, and their more evolved counterparts, the young supergiants. The combined feature of main sequence stars and blue supergiants (evolved stars at the hot edge of their core He-burning phase) shows up near $V-I \approx 0.0$, while red supergiants appear near $V-I \approx 1.3$. Our deeper ACS data show, as expected, that these sequences extend down to much fainter magnitudes. But more importantly, the ACS data reveal the unmistakable presence of a much older population. AGB and carbon stars are seen at $I = 24$–26, with colors extending from $V-I \approx 1.2$ to as much as $V-I \approx 4.0$. Below $I \approx 26.5$ there is a prominent RGB with a pronounced RGB tip (TRGB).

We used the software developed by one of us (RvdM) and described in Cioni et al. (2000) to determine the TRGB magnitude: $I_{\rm TRGB} = 26.67 \pm 0.02({\rm random}) \pm 0.03({\rm systematic})$. We also determined the color of the TRGB, using a histogram of the star colors in a magnitude range just below the TRGB: $(V-I)_{\rm TRGB} = 1.28 \pm 0.02({\rm random}) \pm 0.03({\rm systematic})$. The systematic errors include the uncertainty introduced by the transformations from the ACS filters to the Johnson-Cousins bands, the algorithmic uncertainties associated with finding a discontinuity in the luminosity function, and the fact that this discontinuity is not infinitely steep due to observational uncertainties.

To fit the RGB we use theoretical isochrones from the Padua group, as compiled and

transformed to the Johnson-Cousins system by Girardi et al. (2002).[1] The models include a simple synthetic scheme for TP-AGB evolution. Their metallicity Z (the mass fraction of metals heavier than helium) samples the range from 0.0001 to 0.03. To constrain the age of the RGB stars with the help of these models we need some independent knowledge of the metallicity and the internal reddening A_V.

If SBS 1415+437 has the same ratio of oxygen to metals as the Sun, then the observed nebular oxygen abundance can be combined with the most up-to-date solar values $12 + \log(\mathrm{O/H})_\odot = 8.66$ and $Z_\odot = 0.0122$ (Asplund, Grevesse & Sauval 2005) to obtain $Z = 0.0010$. However, if the galaxy has the same ratio of iron to metals as the Sun then the implied metallicity is only $Z = 0.0003$, because the HII regions in SBS 1415+437, like other BCDs, are α-enhanced compared to the Sun (T99). Either way, the RGB stars probably formed from gas that was more pristine and less metal-enriched than the present-day gas for which nebular abundances are available. We therefore adopt $Z = 0.0010$ as a fairly firm upper limit to the metallicity of SBS 1415+437.

T99 used the Balmer decrement in a nuclear spectrum to estimate an internal reddening $A_V = 0.25$, corresponding to $E(V-I) = 0.13$. We adopt this as an upper limit to the average extinction suffered by RGB stars, for three different reasons: (i) the nebular gas is usually associated with SF regions, which tend to be inherently more dusty than the regions in which older stars reside (as demonstrated explicitly for the case of the LMC; Zaritsky 1999); (ii) the nuclear regions of galaxies often tend to be the most dusty ones; and (iii) the T99 estimate did not account for possible Balmer absorption contamination from an underlying evolved population. Given the upper limit to $E(V-I)$, and taking into account the random and systematic errors, we infer that the true unreddened color of the TRGB must be in the range $1.10 \leq (V-I)_{\mathrm{TRGB}} \leq 1.33$.

Figure 3 shows contours of the predicted TRGB color in the parameter space of metallicity vs. age. The TRGB becomes redder if either age or metallicity is increased. The filled green area shows the region bounded by the available constraints on Z and $(V-I)_{\mathrm{TRGB}}$. It shows that the age of the observed red giants might be anywhere between $\sim 1.3\,\mathrm{Gyr}$ and the Hubble time. To obtain the youngest ages, one must assume that the dust extinction A_V and metallictity Z are at the upper extremes of their allowed ranges.

For reference it is useful to consider one particular model in more detail. Let us choose the model with $Z = 0.0010$ and $A_V = 0$ and call this the "standard" model. To reproduce

[1]The models and their properties are listed in rows 2–8 of Table 1 in Girardi et al. (2002). They are available electronically at http://pleiadi.pd.astro.it/ . The models all have solar abundance ratios; α-enhanced models are more appropriate for BCDs, but are not generally available at the metallicities relevant for BCDs.

the observed color of the TRGB in this model, the age of the RGB stars must be 2.2 Gyr. The absolute magnitude of the TRGB at this age is $M_{I,\mathrm{TRGB}} = -3.99$. This implies a distance modulus $m - M = 30.66$ ($D \approx 13.6$ Mpc). Figure 2a overplots in red the RGB for the 2.2 Gyr isochrone on top of the data, showing an excellent fit. Figure 2b plots isochrones for other ages in the standard model and shows good qualitative agreement also with the other sequences in the observed CMD. Only the carbon star sequence is not well fit, which is a known shortcoming of these stellar evolution models (Marigo, Girardi & Chiosi 2003).

The inferred TRGB distance modulus for the standard model has a systematic error of at least 0.1 mag due to uncertainties in the evolutionary calculations (e.g., Bellazzini et al. 2004). There is an additional systematic uncertainty associated with the unknown dust extinction $0 \leq A_I \lesssim 0.12$. So overall the result agrees well with the value $m - M = 30.42$ implied by straightforward application of the Hubble law. It also agrees with a simple estimate that can be obtained from the carbon stars. Their modal I-band magnitude is $I = 25.78 \pm 0.04$ (see Fig. 2). If we assume that these carbon stars are on average equally luminous as those in the LMC at $m - M = 18.5 \pm 0.1$ (van der Marel & Cioni 2001), then SBS 1415+437 must have $m - M = 30.45 \pm 0.11$(random). The age and metallicity dependence of the carbon star magnitudes is poorly known, but probably adds at least ~ 0.2 mag of systematic error to this estimate. Either way, these agreements provide an independent reason why the RGB stars in SBS 1415+437 cannot be younger than ~ 1.3 Gyr. Not only would such young RGB stars have a TRGB that is bluer than observed, but $M_{I,\mathrm{TRGB}}$ would also be up to 2 mag fainter than the usual value (Barker, Sarajedini & Harris 2004) since in the youngest RGB stars He ignites in non-degenerate cores. The implied TRGB distance modulus of SBS 1415+437 would then be quite inconsistent with the values implied by the Hubble law and the observed carbon star brightnesses. Moreover, for ages below ~ 1.3 Gyr the RGB and its tip cease to be well-defined features in the CMD, in conflict with the observed CMD morphology in Figure 2a.

At $I = 27$ the observed RGB has a Gaussian $V - I$ dispersion of 0.19 (see Fig. 2a), which is twice the median photometric error. This might be because the photometric random errors underestimate the true errors. Alternatively, the observed RGB width may indicate an intrinsic spread in properties. For the standard model, the observed RGB width can be reproduced either with a Gaussian dispersion of 0.60 dex in Z or 0.31 dex in age. A spread in the extinctions $E(V-I)$ towards individual stars might also contribute towards the observed width.

The mass in evolved stars can be estimated using the best-fitting (2.2 Gyr) isochrone in the standard model. For a Salpeter Initial Mass Function (IMF) from 0.1–100 $\mathrm{M}_\odot$, only 1 in 2.4×10^4 randomly drawn stars is observed in a 1 magnitude range below the TRGB.

Since we actually observe ~ 2500 stars there (with $1.0 \leq V-I \leq 1.5$) the galaxy must have $\sim 6 \times 10^7$ stars on this isochrone. The associated mass is $2.1 \times 10^7\,\mathrm{M}_\odot$ (the average mass per star is $0.35\,\mathrm{M}_\odot$ for the adopted IMF). The mass increases if the RGB stars are assumed to be older. T99 estimated the mass in young stars ($\lesssim 100\,\mathrm{Myr}$) to be only $1.2 \times 10^6\,\mathrm{M}_\odot$. Detailed modeling of the SF history will be presented in a forthcoming paper, but preliminary results broadly confirm that at least 80% of the stellar mass of SBS 1415+437 resides in stars with ages $\gtrsim 1.3$ Gyr. The follow-up paper will also address the variations in the SF history along the main body of the galaxy, which was previously found by T99 to be quite non-homogeneous. Here we simply note that the RGB stars seen in the CMD of Figure 2 are in fact spread over the entire galaxy, and are not just found exclusively in one particular region.

4. Conclusions & Discussion

We have used HST/ACS to detect AGB and RGB stars in the metal-poor BCD SBS 1415+437. The data imply that most of the stellar mass of this galaxy resides in stars older than ~ 1.3 Gyr. It was proposed previously that this galaxy (T99), and others like it (IT99), did not form stars more than ~ 100 Myr ago. This was based primarily on interpretation of integrated spectra and heavy element abundances in HII regions. Our results show that such data should be used with caution when addressing the SF history of the underlying stellar population.

Our results add to the growing list of low-metallicity galaxies in which an RGB has been detected with HST, including the BCDs I Zw 36 (12+log(O/H) = 7.77; $D = 5.9$Mpc; Schulte-Ladbeck et al. 2001), VII Zw 403 ($12 + \log(\mathrm{O/H}) = 7.69$; $D = 4.5$ Mpc; Schulte-Ladbeck et al. 1999) and UGC 4483 ($12 + \log(\mathrm{O/H}) = 7.54$; $D = 3.2$ Mpc; Dolphin et al. 2001; Izotov & Thuan 2002), and the Local Group dwarf irregular galaxies Leo A ($12 + \log(\mathrm{O/H}) = 7.30$; Tolstoy et al. 1998, Schulte-Ladbeck et al. 2002) and SagDIG ($12 + \log(\mathrm{O/H}) = 7.26$–$7.50$; Momany et al. 2005). The situation for the most metal-poor BCD, I Zw 18, has been less clear-cut, possibly because it is more metal-poor than any other galaxy studied ($12 + \log(\mathrm{O/H}) = 7.18 \pm 0.01$; IT99) or because of its larger distance ($D \approx 15$ Mpc). Early HST images did reveal asymptotic giant branch (AGB) stars in I Zw 18 (e.g., Aloisi, Tosi & Greggio 1999; Östlin 2000), but Izotov & Thuan (2004) did not detect an RGB in more recent deeper imaging with ACS. However, the latter result has now been challenged by Momany et al. (2005) based on a better photometric analysis of the same data. They show that many red sources do exist at the expected position of an RGB, and that their density in the CMD drops exactly where a TRGB would be expected. Additional HST/ACS data

of I Zw 18 may be needed for a conclusive understanding of its SF history. But either way, the preponderance of the evidence now seems to suggest that the local Universe simply may not contain any galaxies that are currently undergoing their first burst of star formation.

Support for proposal 9361 was provided by NASA through a grant from STScI, which is operated by AURA, Inc., under NASA contract NAS 5-26555. E. Smith and T. Brown are acknowledged for their advice on the photometric reduction of crowded fields observed with ACS.

REFERENCES

Aloisi, A., Tosi, M., & Greggio, L. 1999, AJ, 118, 302

Asplund, M., Grevesse, N., & Sauval, J. 2005, in "Cosmic abundances as records of stellar evolution and nucleosynthesis", F.N. Bash & T.G Barnes, eds., ASP, in press [astro-ph/0410214]

Bellazzini, M., Ferraro, F. R., Sollima, A., Pancino, E., & Origlia, L. 2004, A&A, 424, 199

Babul, A., & Rees, M. J. 1992, MNRAS, 255, 346

Barker, M. K., Sarajedini, A., & Harris, J. 2004, ApJ, 606, 869

Cioni, M. R., van der Marel, R. P., Loup, C., & Habing, H. J. 2000, A&A, 359, 601

Dolphin, A. E., et al. 2001, MNRAS, 324, 249

Girardi, L., Bertelli, G., Bressan, A., Chiosi, C., Groenewegen, M.A.T., Marigo, P., Salasnich, B., & Weiss, A. 2002, A&A 391

Izotov, Y. I., & Thuan, T. X. 1999, ApJ, 511, 639 (IT99)

Izotov, Y. I., & Thuan, T. X. 2002, ApJ, 567, 875

Izotov, Y. I., & Thuan, T. X. 2004, ApJ, 616, 768

Marigo P., Girardi L., Chiosi C., 2003, A&A, 403, 225

Momany, Y., et al. 2005, A&A, in press [astro-ph/0505399]

Östlin, G. 2000, ApJ, 535, L99

Riess, A., & Mack, J. 2004, ACS Instrument Science Report 2004-006 (Baltimore: STScI)

Schulte-Ladbeck, R. E., Hopp, U., Crone, M. M., & Greggio, L. 1999, ApJ, 525, 709

Schulte-Ladbeck, R. E., Hopp, U., Greggio, L., Crone, M. M., Drozdovsky, I. O. 2001, AJ, 121, 3007

Schulte-Ladbeck, R. E., Hopp, U., Drozdovsky, I. O., Greggio, L., & Crone, M. M. 2002, AJ, 124, 896

Sirianni, M., et al. 2005, PASP, submitted

Stetson, P. B. 1987, PASP, 99, 191

Thuan, T. X. 1991, in Massive Stars in Starbursts, ed. C. Leitherer, N. R. Walborn, T. M. Heckman, & C. A. Norman (Cambridge Univ. Press), 183

Thuan, T. X., Izotov, Y. I., & Foltz, C. B. 1999, ApJ, 525, 105 (T99)

Thuan, T. X., & Martin, G. E. 1981, ApJ, 247, 823

Tolstoy, E., et al. 1998, AJ, 116, 1244

van der Marel, R. P., & Cioni, M.-R. L. 2001, AJ, 122, 1807

Zaritsky, D. 1999, AJ, 118, 2824

This figure is available as a gif file from astro-ph

Fig. 1.— True-color composite image of SBS 1415+437 showing a field of view of 52.5×33.5 arcsec^2 centered on the target. HST/ACS F606W data (V) are shown in blue and F814W data (I) in red. North is at about $-14.6°$ from horizontal. The inset in the bottom right shows a single-band blow-up of a 1×1 arcsec^2 region to give a sense of the amount of crowding and noise. This region is neither a best-case nor a worst-case in terms of crowding, but is fairly typical for the main body of the galaxy.

This figure is available as a gif file from astro-ph

Fig. 2.— (a) CMD of the resolved stellar population of SBS 1415+437. The data are corrected for foreground extinction, but not for possible extinction internal to the galaxy. The median photometric random error as a function of I-band magnitude is indicated on the right. The dashed curve provides an estimate of the 50% completeness level. The RGB for an age of 2.2 Gyr is overplotted in red for our "standard model" with metallicity $Z = 0.0010$, no internal extinction, and distance modulus $m - M = 30.66$. (b) Padua model isochrones for the standard model (black) for (roughly from top left to bottom right) log(age) = 6.75, 7.00, 7.25, ..., 9.75, 10.00. The main evolutionary sequences seen in the data are indicated in approximate sense as colored straight lines: main sequence (MS), blue supergiants (BSG), red supergiants (RSG), the red giant branch (RGB) with its tip (TRGB), the asymptotic giant branch (AGB) and carbon stars (AGB stars in which carbon has been dredged up to the surface).

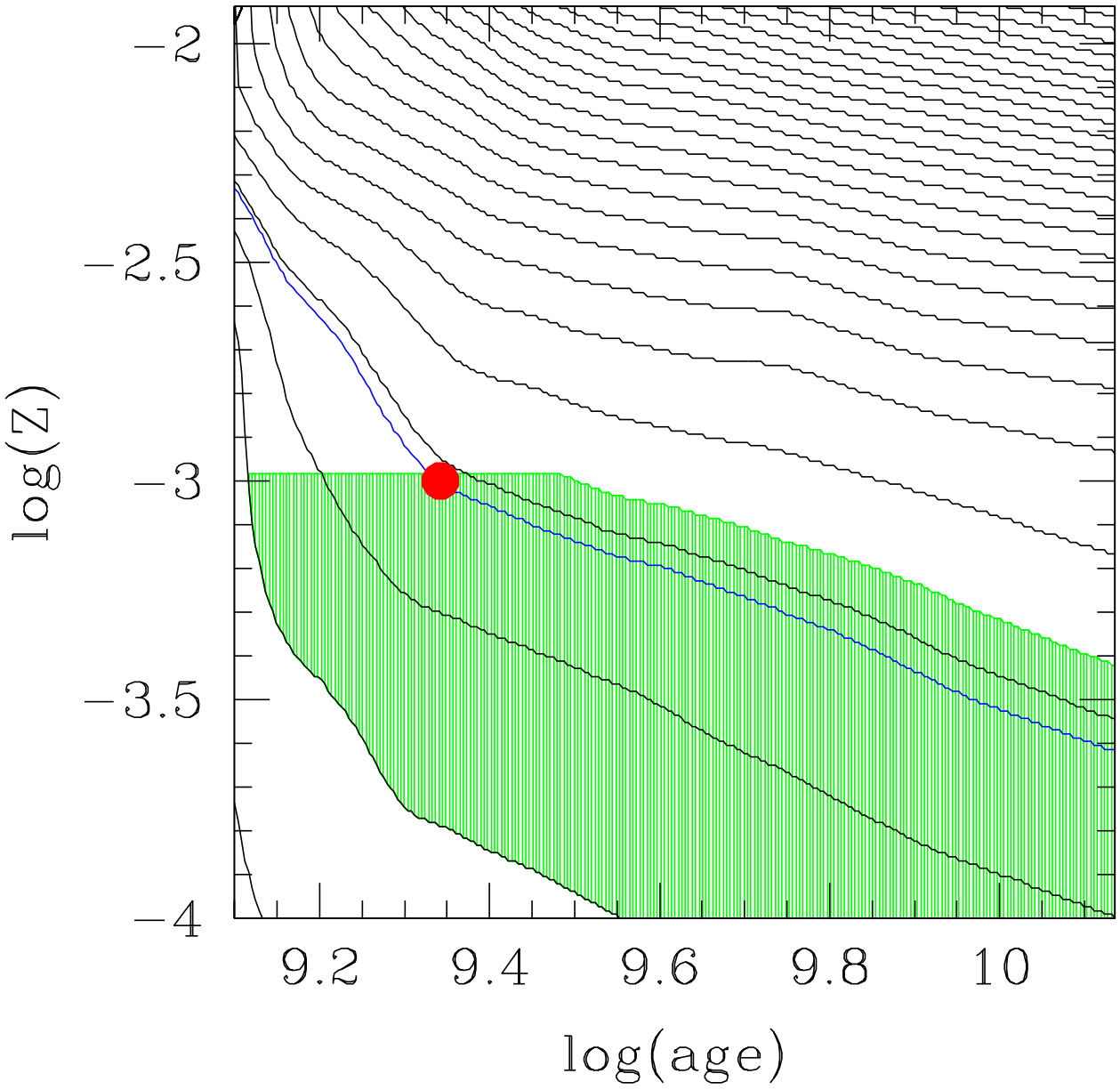

Fig. 3.— Curved solid lines show contours of constant TRGB color in the parameter space of log(Z) vs. log(age). The age is expressed in years. The metallicity Z runs from 0.0001 at the bottom of the plot to 0.0122 (the solar metallicty $Z_{\odot}$; Asplund et al. 2005) at the top of the plot. The contours were calculated from the Padua model isochrones and run from $(V-I)_{\rm TRGB} = 1.0$ in the bottom left to $(V-I)_{\rm TRGB} = 3.6$ in the top right, in steps of 0.1. The blue curve corresponds to the actually observed color $(V-I)_{\rm TRGB} = 1.28$. The red dot on this curve marks the parameter combination for which the RGB is shown in Figure 2a. The green area marks the region in which the RGB stars of SBS 1415+437 must reside, given the available constraints on its metallicity and dust extinction.

This figure "f1.gif" is available in "gif" format from:

http://arXiv.org/ps/astro-ph/0508484v1

This figure "f2.gif" is available in "gif" format from:

http://arXiv.org/ps/astro-ph/0508484v1